Measurement of Shock Wave Rise Times in Metal Thin Films

K. T. Gahagan, D. S. Moore, David J. Funk, R. L. Rabie, and S. J. Buelow
Los Alamos National Laboratory, Los Alamos, New Mexico 87545

J. W. Nicholson
Department of Physics and Astronomy, University of New Mexico, 800 Yale Boulevard NE, Albuquerque, New Mexico 87131
(Received 24 March 2000)

We have measured the rise time of laser-generated shock waves in vapor plated metal thin films using frequency-domain interferometry with subpicosecond time resolution. 10%–90% rise times of <6.25 ps were found in targets ranging from 0.25 to 2.0 μm in thickness. Particle and average shock velocities were simultaneously determined. Shock velocities of ~5 nm/ps were inferred from the measured free surface velocity, corresponding to pressures of 30–50 kbar. Thus, the shock front extends only a few tens of lattice spacings.

PACS numbers: 62.50.+p, 42.87.Bg, 47.40.Nm, 82.40.Fp

I. Introduction.—The dominant mechanisms for coupling of energy into molecular systems, including reactive systems, under shock loading conditions will strongly depend on the structure of the shock. Numerous articles in the literature address this phenomenon from the point of view of the differences in shock wave loading and static loading. Catastrophic shocks [1], equilibrium shocks [2], and many intermediate models [3,4] have been proposed. Certain static high pressure phenomena are reproduced in the shock state—notable among them are first order phase transitions. Shock waves are known to produce the onset of plasticity wherein deviatoric stress components exceed yield strengths. The onset of plasticity is accompanied by large scale atomic level dislocations [5]. Such behavior is influenced, in the case of one-dimensional (1D) shock loading, by the condition of one-dimensional strain. Shock loading provides a nearly instantaneous alteration of material from an initial state to a state of chemical and/or thermodynamic disequilibrium. This altered state is the boundary condition for the relaxation behavior that follows the shock (i.e., plastic flow, chemistry, phase transition, etc.). The degree of disequilibrium is determined by the relative rate of the onset of the altered shock state versus the relaxation time constants—the kinetic coefficients—of the induced processes that seek to return the system to equilibrium. Thus a prelude to any discussion of shock-induced processes requires an elucidation of the shock at the molecular scale.

The most common methods used to determine shock rise times measure the free surface particle velocity as a shock wave exits a target material. These methods include various forms of interferometry (e.g., VISAR, Fabry-Perot, and ORVIS) with time resolutions from a few ns down to 200 ps [6–9]. A novel method utilizing singular value decomposition of coherent anti-Stokes Raman scattering (CARS) spectra for thin anthracene nanogauges, developed by Tas *et al.,* has achieved ~25 ps time resolution (limited by the laser system employed) [10,11]. A more recent spectroscopic method, frequency-domain interferometry, promises subpicosecond time resolution [12,13]. Evans *et al.* [14] have employed this method to measure the average shock velocity and final free surface velocity of aluminum films for laser-driven Mbar shocks. Benuzzi-Mounaix *et al.* [15] have used a variant of this technique, chirped-pulse spectral interferometry, for similar purposes. However, the signal-to-noise level of these measurements was not sufficient to quantify the earliest stages of shock breakout (where the information on the rise time of the shock wave resides). In both cases, no account was made of the pressure and/or temperature dependence of the complex refractive index of the aluminum.

In this paper, we report the first direct measurement of shock-induced free surface acceleration with subpicosecond time resolution for time-resolved characterization of the shock wave rise time. These measurements in metals are a prelude to the application of this technique to reactive molecular systems. We discuss the method used, the results to date, the difficulties of applying this method, and the pitfalls one must avoid to acquire meaningful data.

II. Experiments.—Frequency-domain interferometry was employed to simultaneously measure the dynamic surface motion and reflectance during shock breakout from thin metal films [11–13]. A single 800 nm, $t_p = 130$ fs, 0.7 mJ laser pulse generated by a seeded, chirped pulse amplified Ti:sapphire laser system (Spectra Physics) was used for both shock generation and probing. The shock generating pulse (0.2–0.5 mJ) was focused onto the front side of the target assembly to a spot size of $d_s = 75$ μm. Part of the main pulse (~0.04 mJ) reflected from a beam splitter was passed through an unbalanced Michelson interferometer to produce a pair of probe pulses separated in time by 4–16 ps. These pulses were focused on the back of the target at an angle $\theta = 32.6°$ to a spot size of ~200 μm circumscribing the shocked region. The probe pulses were *s* polarized relative to the plane of incidence. A doubling crystal was optionally inserted before interaction with the target to probe at 400 nm. In all cases, the probe intensity was $<5 \times 10^{11}$ W/cm^2.

We studied polycrystalline aluminum and nickel thin films ranging in thickness from 250 nm to 2 μm produced by vapor deposition onto $\sim 150 \pm 20$ μm thick glass microscope cover slips. The drive pulse was incident through the cover slip onto the absorbing metal film. To improve temporal resolution and simplify modeling, it is desirable to create a planar shock wave parallel to the sample surface. Fortuitously, we found that nonlinear absorption on the passage of the drive beam through the glass substrate acts as an optical limiter, flattening the fluence distribution of the Gaussian input profile. In fact, the rms deviation of the free surface profile was <0.7 nm over a 75 μm diameter central region of the 100 μm total diameter shock. The details of this effect are given in a companion paper [16].

The reflected probe pulses were imaged at $\times 16$ magnification onto the entrance slit of a high resolution imaging spectrograph (Acton model 300i) with a TE-cooled CCD detector (Photometrics model SenSys 1600). The image was oriented with the slit centered along the perpendicular to the probe pulse plane of incidence, providing spatially resolved data at a single pump/probe delay time. Following Geindre *et al.* [13], the relative phase shift between the probe pulses was determined by performing an inverse fast-Fourier transform (IFFT) on the spectral intensity interferogram recorded on the spectrograph CCD. The IFFT is characterized by a central peak with antisymmetric side lobes at $\pm\Delta t$. By assuming identical probe pulses, the $+\Delta t$ side lobe is given by $\sqrt{R(t)R(t-\Delta t)}\,G(t-\Delta t)\exp -i\Delta\Phi$, where $R(t)$ is the time-dependent surface reflectance, $\Delta\Phi$ is the relative phase shift between the pulses, and $G(t)$ is the inverse transform of the individual probe pulses. Dividing this result with a reference shot (taken ~ 1 s prior to the experiment) yields the dynamic phase and reflectance changes in the form $(\sqrt{R(t)R(t-\Delta t)}/R_0)\exp[-i(\Delta\Phi - \Delta\Phi_0)]$, where R_0 is the initial surface reflectance and Φ_0 is a background phase offset associated with changes in the optical path between the reference and experimental shots and is removed using baseline fitting to the unshocked perimeter.

III. Results.—A time profile of the relative phase shift is built up from single shot phase measurements over a range of time delays between the drive pulse and probe pulses, and used to compute the free surface motion of shocked aluminum and nickel thin films. Figure 1 shows the relative phase shift, $\Delta\Phi$, as a function of pump delay time for various nickel films. The targets were each fabricated with a thin (50 nm) region used as a fiducial for measuring the shock breakout time relative to initiation to determine the average shock velocities reported in Table I. Time $t = 0$ in Fig. 1 corresponds to the estimated arrival of the laser pulse at the nickel surface.

To describe the relation between the measured phase profile and the free surface velocity we consider an idealized discontinuous (i.e., zero rise time) shock front for which the free surface velocity rises instantaneously to a final value. The phase profile of such a shock is characterized by a linear rise from zero to a final value proportional to the final free surface velocity during the time interval Δt. The measured phase profiles exhibit similar characteristics, but with gradual rather than instantaneous transitions on the time scales of the measurement, indicative of an observable acceleration of the free surface.

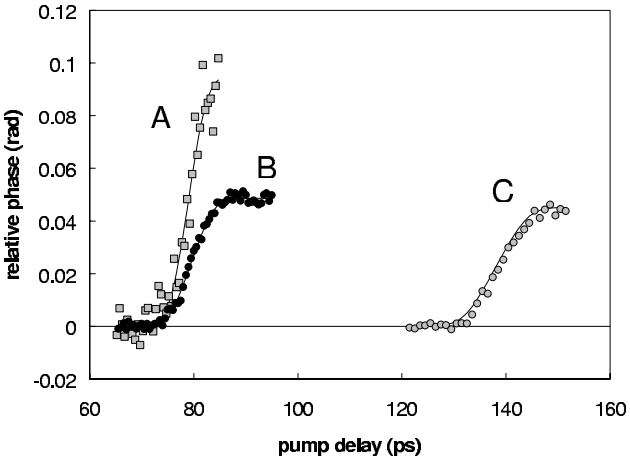

FIG. 1. Spectral interferometric phase (rad) averaged over the central 50 μm of the shock breakout region as a function of time delay (ps) between the pump pulse and first probe pulse for nickel films with (*A*) a 467 nm film probed at $\lambda_{pr} = 400$ nm, $\Delta t = 6$ ps, (*B*) a 467 nm film probed at $\lambda_{pr} = 800$ nm, $\Delta t = 8$ ps, and (*C*) an 839 nm film probed at $\lambda_{pr} = 800$ nm, $\Delta t = 8$ ps. Time $t = 0$ is set by a fiducial measurement of shock breakout from a 50 nm thick region.

To obtain a particle velocity and shock wave rise time, we examined two approaches: (i) assume a hyperbolic tangent form for the free surface velocity, u_{fs}, where τ_{fs} and t_0 are fitting parameters characterizing the free surface velocity profile; (ii) apply a noise filter to obtain a smooth fit to the data, then differentiate to obtain a velocity. In either case, the free surface velocity rise time, which we define as the time it takes for the velocity to go from 10% to 90% of the final free surface velocity, was the same within experimental error. We assume the hyperbolic tangent form in the following discussion.

The final free surface velocity is taken to be twice the final particle velocity of the shock state. This assumes a reflected Hugoniot, or Walsh equation of state, for the rarefaction wave and breakout into air or vacuum. We assume that the rarefaction develops simultaneously with the arrival of the shock wave. That is, as the shock pressure rises incrementally, the rarefaction develops and the free surface accelerates to the velocity corresponding to isentropic relaxation from the shock state. This assumption is supported by the fact that measurements made with the target orientation reversed (i.e., observing the interface between the glass coverslip and metal layer) give an identical rise time within experimental error. If the dynamic response of the free surface deviated significantly from the Walsh equation of state, the difference in interface velocity rise time for these two systems would be large, owing to

TABLE I. Average shock velocity ($\overline{U}_{sh}$), shock velocity at breakout (U_{sh}), final free surface velocity (u_p), hyperbolic tangent time constant for the free surface velocity (τ_{fs}), and 10%–90% shock wave rise time (τ_{sh}) for nickel and aluminum films of various thickness probed at two different wavelengths, λ_{pr}.

Sample	λ_{pr} (nm)	$\overline{U}_{sh}$ (nm/ps)	U_{sh}[a] (nm/ps)	u_p (nm/ps)	τ_{fs} (ps)	τ_{sh} (ps)
1000 nm aluminum (*D*, *E*)	400	–	5.72 ± 0.02	0.29 ± 0.02	2.32 ± 0.40	5.34 ± 0.92
750 nm aluminum	800	–	5.76 ± 0.01	0.30 ± 0.01	2.3 ± 0.4	5.3 ± 1
2000 nm aluminum	800	–	5.59 ± 0.01	0.18 ± 0.01	2.4 ± 0.4	5.5 ± 1
250 nm nickel	800	6.28 ± 0.5	5.13 ± 0.01	0.36 ± 0.01	2.4 ± 1	5.5 ± 1
467 nm nickel (*A*)	800	6.62 ± 0.4	4.90 ± 0.01	0.22 ± 0.01	2.54 ± 0.73	5.84 ± 1.68
839 nm nickel (*C*)	800	6.15 ± 0.39	4.80 ± 0.02	0.14 ± 0.01	2.71 ± 1.10	6.23 ± 2.53
467 nm nickel (*B*)	400	–	5.03 ± 0.06	0.30 ± 0.04	2.57 ± 1.42	5.91 ± 3.24

[a]Note: $U_{sh} = 4.60 + 1.437u_p$ for nickel, and $U_{sh} = 5.35 + 1.34u_p$ for aluminum (see Ref. [16]).

the large difference in impedance matching. This assumption is in close agreement with results from large scale molecular dynamics simulations [17].

In this case, we may approximate the time-dependent particle velocity as half the free surface velocity. Thus, the free surface velocity, particle velocity, and shock velocity are all characterized by the single time constant τ_{fs}, where $u_{fs} = u_p(1 + \tanh[(t - t_0)/\tau_{fs}])$. Values are reported in Table I for a range of film thicknesses.

Measurements on a 1 μm thick aluminum film are shown in Fig. 2. Sample *D*, probed at 400 nm, exhibits a qualitatively similar phase profile compared to the nickel samples. However, the phase profile for sample *E*, probed at 800 nm, shows a distinct negative phase shift coincident with shock breakout. This effect is mirrored 8 ps later as the second probe pulse strikes the surface during the negative phase shift. The phase change then settles to the same end value as for sample *D*. This behavior suggests that the effect is transient with a time scale similar to the rise time of the free surface velocity. We attribute the negative phase contribution in aluminum to the presence of a strong 1.5 eV interband transition at 800 nm, which is known to shift toward higher frequency with pressure [18]. A simple model assuming a change in complex refractive index proportional to the acceleration of the free surface fits data for aluminum samples well for a range of incident angles and both *s* and *p* polarization. A more detailed analysis of this effect is reported elsewhere [19]. The values in Table I for aluminum probed at 800 nm include a correction using this model.

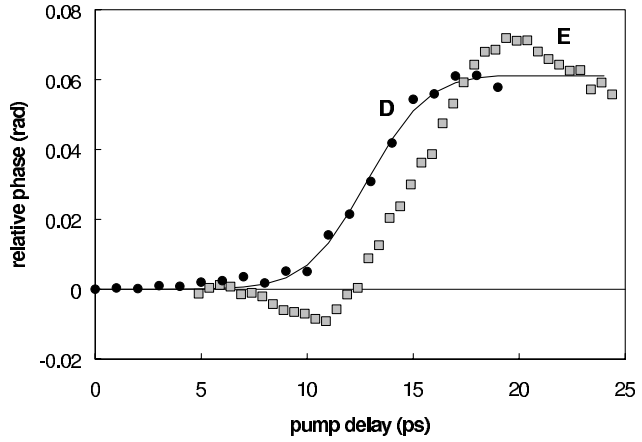

FIG. 2. Spectral interferometric phase averaged over the central 50 μm of the shock breakout region as a function of time delay between the pump pulse and first probe pulse for a 1 μm thick aluminum film probed with (*D*) $\lambda_{pr} = 400$ nm, $\Delta t = 6$ ps, and (*E*) $\lambda_{pr} = 800$ nm, $\Delta t = 8$ ps. The negative phase shift in sample *E* may be associated with a pressure-dependent shift of the 800 nm interband absorption.

In contrast to aluminum, a small *positive* transient optical phase shift is observed in nickel samples probed at 800 nm near the quasipolarizing angle [19]. The aforementioned model proposed for aluminum does not fit the nickel data as well, and we are investigating other possible reasons for this failure such as the presence of voids and differences in optical skin depth. As such, the values reported in Table I for nickel do not include an optical phase contribution in the fitting to a hyperbolic tangent form for the free surface velocity.

The standard deviation of our phase measurements at early time (prior to shock breakout) is typically $\sigma_0 \leq 2$ mrad for 800 nm probes, where the spectrometer throughput is optimized. This value is consistent with estimates of the fundamental instrumental limitations of the technique calculated by Geindre *et al.* [13]. The fundamental time resolution is on the order of the probe pulse width of 130 fs. We now consider experimental factors limiting the resolution of our measurements.

The free surface velocity profile is constructed from individual shots at each delay time. Thus, the shot-to-shot timing jitter owing to variations in shock velocity or average sample thickness will convolve the phase data along the time axis. For example, a shock propagating through 1 μm of aluminum at ~7 nm/ps will reach the back surface in 142.8 ps. A variation as small as 2% in thickness or velocity will effectively smooth the phase profile over a 3 ps time interval. Such a convolution will be most apparent when $d\Phi/dt$ is greatest. By comparing the standard deviation of the phase at early times with the increased

standard deviation in the region of the steepest rise in phase, we are able to set an upper limit on the shot-to-shot timing jitter of ~340 fs, slightly larger than the probe pulse width and significantly smaller than the measured free surface rise time.

Surface roughness may also affect the resolution of the phase profile. For example, an infinitesimally thin shock propagating at 6–7 nm/ps will take ~3 ps to traverse a surface with an rms roughness of just 20 nm. We estimate the rms surface roughness for our films at <5 nm from atomic force microscopy profile measurements, corresponding to a resolution of ~1 ps. It may be advantageous to probe through the glass layer where the interface roughness is smaller (~1 nm rms) than at the free surface of a vapor deposited film. We performed this experiment as well and find no measurable difference in the rise time.

A final point concerns the expected and observed structure of the pressure wave. For example, at 50 kbars we may expect both an elastic wave and plastic wave to be present depending upon the run time of the shock wave. A 1D finite-difference hydrocode calculation (CTH, Sandia National Laboratory) for impulsive shock in aluminum, similar to our experimental conditions, predicts an elastic precursor or shoulder prior to the main shock wave. Indeed, the aluminum data probed at 400 nm (sample *D*) in Fig. 2 shows a small positive phase shift prior to arrival of the main pressure pulse. It is possible that this initial phase shift is associated with an elastic wave. However, given that we have also observed strong phase shifts from pressure-related optical effects, we are reluctant to make this assignment at present.

IV. Conclusions.—We have presented spectral interferometric measurements of free surface velocity for laser-generated shock waves in aluminum and nickel thin films. Values of <6.25 ps were obtained with an estimated resolution of slightly less than 1 ps limited mainly by the surface roughness of the metal films. These very short rise times suggest that the thickness of these shocks is a few tens of lattice spacings. This may have implications for reaction chemistry in energetic materials under similar shock loading conditions such as direct pumping into transition states. In addition, we have observed a strong influence on phase measurements of the dynamic complex refractive index probing at 800 nm in aluminum. This effect is concurrent with the motion of the free surface in the first few picoseconds of shock breakout and possibly later, depending on shock conditions. Thus, any optical technique performed at this wavelength which attempts to obtain subpicosecond time resolution of early-time shock breakout, including previous spectral interferometric measurements [13,14], should account for this effect.

[1] R. A. Graham, B. Morosin, Y. Horie, E. L. Venturini, M. Boslough, M. J. Carr, and D. L. Williamson, *Shock Waves in Condensed Matter,* edited by Y. M. Gupta (Plenum, New York, 1986), pp. 693–711.

[2] W. Fickett and W. Davis, *Detonation* (University of California Press, Berkeley, 1979).

[3] A. Tokmakoff, M. D. Fayer, and D. D. Dlott, J. Phys. Chem. **97**, 1901 (1993).

[4] C. M. Tarver, J. Phys. Chem. **A101**, 4845 (1997).

[5] B. L. Holian and P. S. Lomdahl, Science **280**, 2085 (1998).

[6] L. M. Barker and R. E. Hollenbach, Rev. Sci. Instrum. **36**, 1617 (1965).

[7] M. Durand, P. Laharrague, P. Lalle, A. Le Bihan, J. Morvan, and H. Pujols, Rev. Sci. Instrum. **48**, 275 (1977).

[8] D. D. Bloomquist and S. A. Sheffield, J. Appl. Phys. **54**, 1717 (1983).

[9] W. F. Hemsing, in *Proceedings of the Eighth International Symposium on Detonation, Naval Surface Weapons Center NSWC MP 86-194* (White Oak, Silver Spring, MD, 1985), p. 468.

[10] G. Tas, J. Franken, S. A. Hambir, D. E. Hare, and D. D. Dlott, Phys. Rev. Lett. **78**, 4585 (1997).

[11] G. Tas, S. A. Hambir, J. Franken, D. E. Hare, and D. D. Dlott, J. Appl. Phys. **82**, 1080 (1997).

[12] E. Tokunaga, A. Terasaki, and T. Kobayashi, Opt. Lett. **17**, 1131 (1992).

[13] J. P. Geindre, P. Audebert, A. Rousse, F. Fallis, J. C. Gauthier, A. Mysyrowicz, A. Dos Santos, G. Hamoniaux, and A. Antonetti, Opt. Lett. **19**, 1997 (1994).

[14] R. Evans, A. D. Badger, F. Falliès, M. Mahdieh, T. A. Hall, P. Audebert, J.-P. Geindre, J.-C. Gauthier, A. Mysyrowicz, G. Grillon, and A. Antonetti, Phys. Rev. Lett. **77**, 3359 (1996).

[15] A. Benuzzi-Mounaix, M. Koenig, J. M. Boudenne, T. A. Hall, D. Batani, F. Scianitti, A. Masini, and D. Di Santo, Phys. Rev. E, Rapid Commun. **60**, R2488 (1999).

[16] D. S. Moore, D. J. Funk, K. T. Gahagan, R. L. Rabie, S. J. Buelow, and T. Lippert (to be published).

[17] Brad Holian (private communication).

[18] H. Tups and K. J. Syassen, J. Phys. F **14**, 2753 (1984).

[19] D. J. Funk, D. S. Moore, K. T. Gahagan, R. Rabie, and S. J. Buelow (to be published).